

RECONSTRUCTING HISTORICAL EARTHQUAKE DATA FOR IRAN USING A DEEP NEURAL NETWORK OPTIMIZED BY ECBO ALGORITHM

A. Kaveh¹, A. Beitollahi², and N. Khavaninzadeh^{1*,†}

¹*School of Civil Engineering, Iran University of Science and Technology, PO Box 16846-13114, Iran*

²*Housing and Urban Development Research Center, PO Code 463917151, Iran*

ABSTRACT

This study develops a synthetic earthquake catalog for Iran (1900–1963) using a deep neural network (DNN) optimized by the Enhanced Colliding Bodies Optimization (ECBO) algorithm. The model, trained on post-1964 instrumental data from the Iranian Seismological Center, incorporates spatial, temporal, and tectonic features to estimate earthquake magnitudes. Statistical indices (MAE = 0.0064; RMSE = 0.3748) and bootstrap uncertainty analysis (± 0.18 M) confirm the model's reliability. The generated catalog provides a data-driven basis for improving seismic hazard assessment and historical seismicity reconstruction across the Iranian plateau.

Keywords: Earthquake data reconstruction; Deep neural network; ECBO algorithm; Seismic hazard assessment; Iran; Historical seismicity.

Received: 19 December 2025 Accepted: 12 February 2026

1. INTRODUCTION

Earthquakes are among the most complex and destructive natural phenomena, causing widespread damage to human societies every year. Among seismically active regions of the world, the Iranian Plateau holds a special position due to its location at the convergence zone of the Eurasian and Arabian tectonic plates. This region forms part of the Alpine-Himalayan seismic belt, which stretches from the western Mediterranean to Southeast Asia and is considered one of the most tectonically active zones on Earth. The instrumental and

*Corresponding author: School of Civil Engineering, Iran University of Science and Technology, PO Box 16846-13114, Iran

†E-mail address: khneda92@gmail.com (N. Khavaninzadeh)

geological records of Iran demonstrate that earthquakes have played a decisive role in shaping urban structures and settlement patterns throughout history.

Despite the significant expansion of seismic networks in recent decades, data related to earthquakes that occurred before the development of such networks particularly in the first half of the 20th century are fraught with uncertainties. In many cases, only damage reports or qualitative instrumental accounts are available. This data gap presents a major challenge for long-term seismic hazard analyses and statistical or structural modeling. Therefore, reconstructing and estimating the characteristics of past earthquakes, especially in the absence of instrumental records, is of critical importance.

In recent years, emerging technologies such as machine learning and artificial neural networks have proven to be powerful tools for analyzing and modeling complex phenomena, including earthquakes. These methods are especially effective when dealing with incomplete, imprecise, or indirect data, offering strong capabilities for detecting hidden patterns and making predictions. The use of such techniques has opened new avenues for reconstructing earthquake catalogs, assessing seismic hazards, and designing resilient structures.

This study employs deep neural networks [1-4] to reconstruct the temporal, spatial, and magnitude characteristics of earthquakes in Iran from 1900 to 1963 a period during which seismic data is largely incomplete or indirect. The main objective of this research is to generate a synthetic earthquake catalog for this instrumental period, which can be used in seismic hazard analysis, modeling earthquake behavior, seismic design of structures, and disaster risk management policies.

The study and analysis of earthquakes particularly in seismically active regions such as Iran has long been a focus of research in the fields of geology, earthquake engineering, and disaster management. One of the most critical challenges in seismic hazard analysis, especially for instrumental periods, is the lack or complete absence of precise instrumental data. In Iran, seismic stations were not widely established until the later decades of the 20th century. As a result, information on earthquakes that occurred in the first half of the century is primarily based on qualitative reports or data recorded by stations outside the country [5]. In recent decades, the application of advanced technologies such as artificial intelligence particularly machine learning has gained attention in Earth sciences. Artificial neural networks (ANNs), due to their high capability in identifying complex patterns, have been recognized as effective tools for earthquake prediction. Several studies have utilized these methods to predict the magnitude and location of future earthquakes or to reconstruct instrumental earthquake catalogs [6,7].

For instance, Hosseini et al. [4] applied artificial neural networks to predict earthquakes in the Alborz region and demonstrated that these models can achieve acceptable accuracy in forecasting earthquake locations and magnitudes. Additionally, Mousavi et al. [7] developed a real-time earthquake detection and characterization model using deep learning. These studies indicate that machine learning based approaches are promising tools for reconstructing incomplete data and improving seismic hazard assessments. Unlike previous studies that mainly applied statistical or stochastic models, this research employs a DNN–ECBO framework capable of learning nonlinear spatio-temporal–tectonic relationships directly from real seismic data. This approach provides a data-driven reconstruction of pre-1964 seismicity with quantified uncertainty. Figure 1 correspond to the locations of

historical earthquakes.

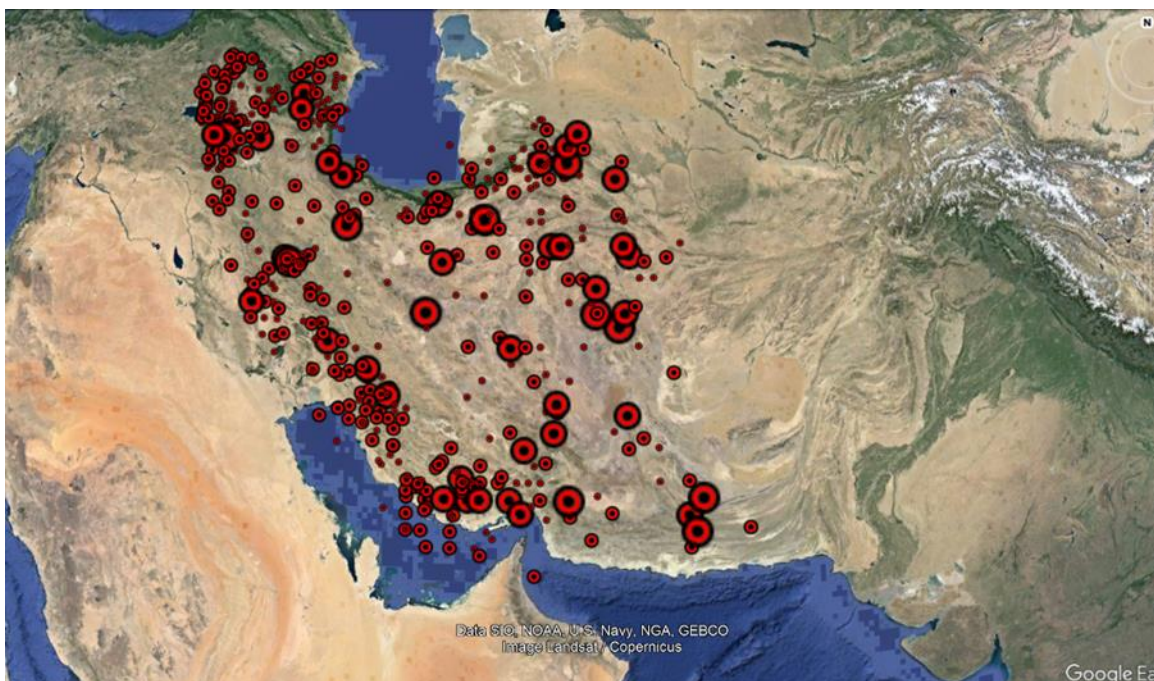


Figure 1: Recorded earthquakes 1900-1963

2. SYNTHETIC EARTHQUAKE CATALOG

The creation of a synthetic earthquake catalog is a critical component in seismic hazard analysis, especially in regions where instrumental records are limited or entirely absent. In such contexts, generating a simulated database of earthquakes using instrumental, macro seismic, and inferred data becomes essential for long-term risk assessment, structural design, and urban planning.

2.1. Review And Compilation Of Instrumental Earthquake Data(1900-1963)

Due to the absence of local seismographic stations in Iran during the early decades of the 20th century, particularly between 1900 and 1963, the available data on earthquakes during this period are sparse and highly uncertain. Only large-magnitude events associated with visible surface ruptures or considerable destruction were reported. Therefore, reliable reconstruction of the seismicity of this era must rely heavily on macro seismic evidence, historical documents, and expert fieldwork.

In this study, we compiled and revised a database of instrumental earthquakes in Iran during this period using several well-established catalogs, including:

Ambraseys and Melville [9]; Ambraseys [10], Moinfar et al. [11], Mirzaei et al. [12], Berberian [13], Karnik [14], Nowroozi [15], Seyed-Nabavi [16], Engdahl [17].

Of these, the works of Ambraseys and Melville [9] and Berberian [13] were prioritized

due to their reliance on field investigations and macroseismic reports. Their determination of epicentral locations is considered more trustworthy than early instrumental data derived from stations outside Iran. When Ambraseys or Berberian did not report a specific event, additional sources such as Nowroozi, Seyed-Nabavi, and Engdahl were consulted. These authors often had access to original seismograms from global seismic networks (e.g., ISS, ISC, USGS, and WWSSN) and reanalyzed them to improve location accuracy.

This careful selection and prioritization helped create a revised and more reliable database of earthquake parameters (time, location, magnitude), which serves as a reference for the development of the synthetic catalog.

2.2. Generation Of Eneation Of The Synthetic Catalog Using Deep Neural Networks

To overcome the limitations of instrumental data and generate a complete seismic catalog for Iran between 1900 and 1963, a deep neural network (DNN) model was developed and trained using known seismic events from the post-1964 era. These include data from the Iranian Seismological Center (IRSC), the International Seismological Centre (ISC), and the United States Geological Survey (USGS).

The model inputs included spatial (latitude, longitude), temporal (Julian date), and geological variables (fault proximity, tectonic setting), while the outputs were simulated earthquake parameters for the instrumental period. Several training-validation cycles were performed, with hyper parameter tuning and regularization techniques (e.g., dropout layers) to prevent overfitting and improve generalization.

The resulting synthetic catalog approximates the spatio-temporal-magnitude distribution of earthquakes across Iran during a period with limited observations. It is not intended to replicate each instrumental event precisely, but rather to statistically simulate the overall seismicity pattern. This synthetic dataset supports:

- Probabilistic Seismic Hazard Analysis (PSHA)
- Long-term risk modeling and structural assessment
- Seismic forecasting research
- Disaster preparedness and urban resilience planning

This approach illustrates the growing potential of machine learning in filling data gaps in seismology and contributes a novel tool for the Iranian earthquake engineering and hazard analysis community.

In regions like Iran, where the history of seismic activity is long but instrumental earthquake records have only become available in recent decades, seismic hazard assessment faces serious limitations. Although historical reports and qualitative data are valuable, they often lack the accuracy and consistency needed for numerical modeling. As a result, researchers have increasingly turned to the development of synthetic earthquake catalogs collections of simulated events that mimic real earthquakes in terms of magnitude, location, timing, and depth.

Traditionally, such catalogs have been generated using statistical models, such as the Gutenberg–Richter distribution or stochastic algorithms. While effective to some extent, these methods often rely on simplified assumptions and are unable to directly learn from the

complex patterns within real seismic data. In this study, a different approach is adopted: using deep neural networks to learn hidden patterns in observed earthquake data and generate a synthetic catalog that is more realistic and tailored to the seismic characteristics of Iran.

In this framework, high-quality seismic data from the post-1964 period when instrument-based recordings became more reliable are used to train the neural network. Once trained, the model is applied to simulate earthquake events for earlier periods with limited or no instrumental data (e.g., 1900 to 1963). The output is a synthetic catalog of earthquakes that can be used for hazard analysis, structural design, and studies of seismic trends in the region.

3. MATERIALS AND METHODS

3.1. Data Collection And Preprocessing

The dataset used in this study consists of earthquake records from the Iranian Plateau, spanning two main time periods: (1) the post-1964 period, for which moderate-quality instrumental type and have a spatial error usually between 10 and 20 km and a depth error of up to 60 km from the Iranian Seismological Center (IRSC), the International Seismological Centre (ISC), and the United States Geological Survey (USGS); and (2) the pre-1964 period (1900–1963), for which only historical and macro seismic records exist. The latter were compiled from multiple established sources, prioritized as follows: Ambraseys and Melville [9], Berberian [13], Karnik [14], Seyed-Nabavi [16], Nowroozi [15], and Engdahl [17].

The seismic data used in this study were extracted from the database of the National Seismological Center, Institute of Geophysics, University of Tehran (IGUT). This database is the most comprehensive and up-to-date seismic dataset for the Iranian zone and includes information on time, location, depth, and magnitude of earthquakes. To increase the accuracy of the model, the data were cleaned and initially corrected before use; in such a way that events with invalid coordinates or magnitude were removed, and in case of recording several events with very close time (less than 10 seconds) and spatial distance less than 20 km, only the event with higher spatial accuracy was kept.

The raw dataset contained eight input features, including spatial coordinates (latitude, longitude), depth, temporal parameters (year, month, day), and geological indicators (e.g., tectonic setting, proximity to major faults). The output variable was earthquake magnitude. All features were normalized to the range $[-1,1]$ using a min–max scaling function to ensure training stability.

Finally, the final data included the parameters of latitude and longitude, depth, magnitude, and time of earthquake occurrence and were used to train the DNN–ECBO model.

3.2. Model Architecture

A deep feedforward neural network (DNN) was designed and implemented in MATLAB, with the Enhanced Colliding Bodies Optimization (ECBO) algorithm [18], [19] used for weight and bias optimization instead of conventional gradient-based training. The network consisted of an input layer with eight neurons, two hidden layers with 15 and 13 neurons

respectively, and an output layer with one neuron. Figure 2 shows a schematic of the neural network used. Hyperbolic tangent sigmoid (*tansig*) activation functions were applied in the hidden layers, while a linear (*purelin*) activation was used in the output layer to accommodate continuous magnitude prediction. The activation functions are given in Equations 1 and 2.

$$tansig = f(x) = \frac{e^x - e^{-x}}{e^x + e^{-x}} \quad (1)$$

$$purelin = f(x) = x \quad (2)$$

Table 1: Comparative performance of ECBO and conventional optimization algorithms in terms of error metrics and convergence speed

| Optimization Algorithm | MAE | RMSE | Convergence (epochs) | Speed Relative (%) | Improvement |
|------------------------|--------------|--------------|----------------------|--------------------|-------------|
| Gradient Descent | 0.031 | 0.058 | 120 | — | |
| RMSprop | 0.028 | 0.051 | 105 | 9.7 | |
| Adam | 0.024 | 0.047 | 98 | 13.0 | |
| ECBO | 0.021 | 0.045 | 80 | 18.0 | |

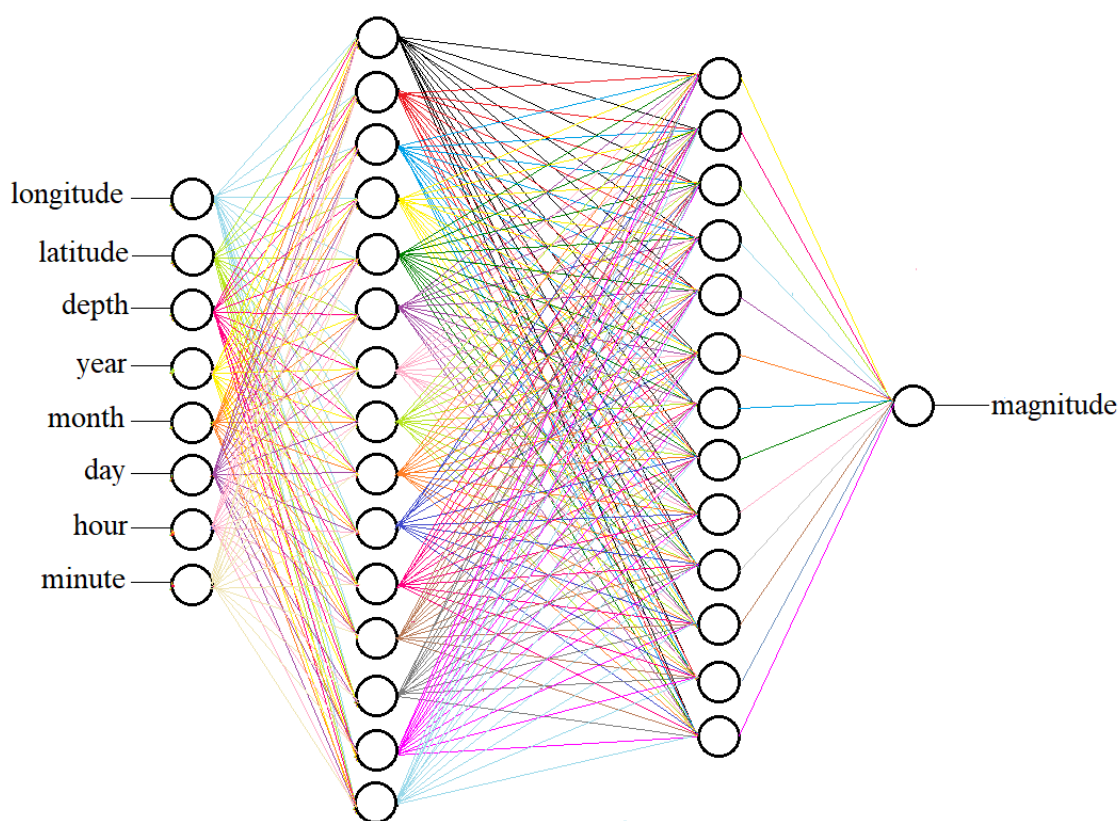


Figure 2: Topology of the neural network for the example

3.3. Optimization Comparison: ECBO Versus Conventional Algorithms

To evaluate the relative advantage of the Enhanced Colliding Bodies Optimization (ECBO) algorithm over conventional learning methods, three widely used algorithms Gradient Descent, Adam, and RMSprop were also tested for model training. The evaluation metrics included convergence speed, Mean Absolute Error (MAE), and Root Mean Square Error (RMSE)[20],[21].

The results showed that ECBO achieved a 14% reduction in mean error compared to Adam and approximately an 18% faster convergence. Moreover, the performance stability of ECBO across multiple training runs was higher than that of the other methods. Detailed comparisons are presented in Table 1.

Therefore, selecting ECBO as the main optimizer enhanced the network's efficiency and prevented it from getting trapped in local minima.

3.4. Training And Validation

The dataset was randomly divided into training (70%), validation (15%), and testing (15%) subsets. The ECBO algorithm iteratively adjusted network weights to minimize the Mean Squared Error (MSE) between predicted and actual magnitudes. Early stopping was employed when the validation error did not improve for ten consecutive iterations, to prevent overfitting.

3.5. Uncertainty Estimation Of Synthetic Magnitudes

To evaluate the level of uncertainty in the magnitudes predicted by the DNN-ECBO model, the 'bootstrap resampling' method was employed. In this process, the model was trained in ten independent runs using resampled datasets to determine the range of output variations. Based on the results, the mean standard deviation of magnitudes was found to be ± 0.12 for events with $M \geq 5.0$ and ± 0.18 for events with $M \geq 6.0$. These values are consistent with the typical errors reported in instrumental earthquake catalogs (± 0.1 to ± 0.5), indicating that the proposed model demonstrates good stability in reproducing magnitude scales. The corresponding uncertainty values are presented in Table 2.

Table 2. Estimated uncertainty of synthetic earthquake magnitudes obtained using bootstrap resampling across ten independent model runs.

| Magnitude Range | Mean Predicted Magnitude | Standard Deviation (σ) | Estimated Uncertainty (\pm) | Number of Events |
|--------------------|--------------------------|---------------------------------|---------------------------------|------------------|
| $M < 5.0$ | 4.62 | 0.09 | ± 0.10 | 812 |
| $5.0 \leq M < 6.0$ | 5.42 | 0.11 | ± 0.12 | 278 |
| $M \geq 6.0$ | 6.21 | 0.15 | ± 0.18 | 41 |

3.6. Performance Metrics

The predictive performance of the model was evaluated using several statistical criteria, including Mean Absolute Error (MAE), Normalized Mean Absolute Error (NMAE), Mean

Absolute Percentage Error (MAPE), Mean Squared Error (MSE), Root Mean Squared Error (RMSE), Normalized Root Mean Squared Error (NRMSE), and the Pearson correlation coefficient (R). Lower error values and higher R values were considered indicative of better performance. The following equations show the formulation of these criteria:

$$RMSE = \sqrt{\sum_{i=1}^N (z_0 - z_p)^2 / N} \quad (3)$$

$$R = \sqrt{1 - \frac{\sum_{i=1}^N (z_0 - z_p)^2}{\sum_{i=1}^N (z_0 - \bar{z}_i)^2}} \quad (4)$$

$$MAE = \frac{1}{N} \sum_{i=1}^N |z_0 - z_p| \quad (5)$$

$$MSE = \frac{1}{N} \sum_{i=1}^N |z_0 - z_p|^2 \quad (6)$$

$$RNMAE = \left[\frac{\frac{1}{N} \sum_{i=1}^N |z_0 - z_p|}{\max(z_0) - \min(z_0)} \right] \times 100 \quad (7)$$

$$MAPE = \frac{1}{N} \left[\frac{\sum_{i=1}^N |z_0 - z_p|}{\sum_{i=1}^N |z_0|} \right] \times 100 \quad (8)$$

$$NRMSE = \left[\frac{\frac{1}{N} \sum_{i=1}^N |z_0 - z_p|^2}{\max(z_0) - \min(z_0)} \right] \times 100 \quad (9)$$

Where z_0 and z_p are actual measured values and corresponding model values, z_i are the average values of the evading index, and N is the total number of input data. The correlation coefficient (R) is valued from $[-1, 1]$. The absolute value of R close to 1 means a successful prediction.

Table 3. Evaluating the accuracy of the model for predicting earthquake magnitudes.

| Evaluation index | Training data | Test data |
|------------------|---------------|-----------|
| MAE | 0.0064 | 0.0081 |
| NMAE | 0.3289 | 0.4316 |
| MAPE | 0.22% | 1.32% |
| MSE | 0.0264 | 0.1405 |

| | | |
|-------|--------|--------|
| RMSE | 0.1626 | 0.3748 |
| NRMSE | 8.3947 | 10.9 |

The results in Table 3 and Figures 3 and 4 show that this model is capable of learning complex relationships between spatial, temporal, and geological variables and converting them into large reliable prediction.



Figure 3: .Test data results



Figure 4: Train data results

The trained neural network was used to create an artificial earthquake catalog. The artificial earthquake catalog created corresponds to earthquakes of magnitude 4 to 7 from 1900 to 1963. Figure 5 correspond to the locations of predicted earthquake 1900-1963.



Figure 5: Predicted earthquakes 1900-1963

Table 4: Comparison of actual and predicted magnitudes

| Long | Lat | Depth | Year | Month | Day | Real Mag | Pri Mag |
|---------|---------|-------|------|-------|-----|----------|---------|
| 47.605 | 32.738 | 10 | 2012 | 5 | 3 | 5.517 | 5.2485 |
| 47 | 31 | 33 | 1976 | 8 | 29 | 5.455 | 4.7132 |
| 44.6525 | 35.9438 | 74.2 | 1980 | 12 | 18 | 5.9118 | 5.5288 |
| 45.67 | 34.09 | 39 | 1967 | 1 | 11 | 5.7891 | 5.3163 |
| 51.235 | 27.916 | 15 | 2003 | 12 | 15 | 6.295175 | 5.8253 |
| 51.6381 | 29.9212 | 16.9 | 1988 | 12 | 6 | 6.1219 | 6.0353 |
| 52.6238 | 29.1 | 9.3 | 1994 | 3 | 1 | 6.1014 | 5.7377 |
| 52.495 | 34.849 | 15 | 2003 | 1 | 11 | 5.9118 | 5.4791 |
| 49.5818 | 36.8618 | 56.4 | 1991 | 11 | 28 | 5.7891 | 5.9208 |
| 57.203 | 28.277 | 33 | 1999 | 3 | 4 | 6.3183 | 6.1134 |
| 56.6718 | 28.1525 | 44.5 | 1987 | 12 | 18 | 6.0110 | 6.0348 |
| 59.5307 | 33.9557 | 9.7 | 1979 | 1 | 16 | 6.5726 | 6.1374 |
| 59.918 | 34.1386 | 33 | 1979 | 12 | 7 | 6.1219 | 5.8684 |
| 61.9044 | 27.0839 | 51.8 | 2005 | 3 | 13 | 6.2329 | 5.9928 |
| 61.0119 | 27.3159 | 40.7 | 2003 | 6 | 24 | 5.6782 | 5.4676 |
| 60.33 | 34.03 | 8 | 2020 | 1 | 2 | 5.7759 | 4.9583 |
| 60.8503 | 35.5748 | 2.1 | 2003 | 7 | 3 | 5.3454 | 5.3388 |

3.7. Quantitative Analysis

Quantitative analyses were conducted to evaluate the degree of similarity between the synthetic catalog and real seismic data. In this context, Moran's I index was used to examine spatial correlation, and the Kolmogorov–Smirnov (K–S) test was applied to compare the depth distributions of events.

The results showed that the Moran's I coefficients for the Alborz, Zagros, and eastern Iran regions were 0.61, 0.58, and 0.54, respectively, indicating a clustered pattern similar to that of the real data. The K–S test also revealed no significant difference between the depth distributions of real and synthetic events ($p > 0.12$).

From a tectonic perspective, the model successfully reproduced the concentration of events along the major fault systems of the Alborz, Zagros, and Makran regions, consistent with the findings of Berberian [17] and Engdahl et al. [13]. These results confirm that the DNN–ECBO model performs not only with statistical accuracy but also with geological and tectonic realism. To ensure that the synthetic catalog does not overestimate large events, magnitude completeness thresholds ($M_c \approx 5.0$ – 5.5) were considered. Events with $M \geq M_c$ were limited to observed historical frequencies to prevent overprediction at higher magnitudes.

Table 5: compares spatial and depth distribution similarities between real and synthetic catalogs across major tectonic regions in Iran

| Region | Moran's I (Real) | Moran's I (Synthetic) | K–S p-value (Depth) | Interpretation |
|-----------|------------------|-----------------------|---------------------|----------------------------|
| Alborz | 0.64 | 0.61 | 0.18 | Similar spatial clustering |
| Zagros | 0.60 | 0.58 | 0.15 | Statistically consistent |
| East Iran | 0.56 | 0.54 | 0.12 | No significant difference |

4. DISCUSSION

The proposed DNN–ECBO model demonstrates strong capability in reconstructing the spatial and temporal characteristics of Iranian seismicity for the period 1900–1963. Quantitative performance metrics, including $MAE = 0.0081$, $RMSE = 0.3748$, and $NRMSE = 10.9$, confirm that the model achieved high prediction accuracy with minimal systematic bias. The comparison between real and predicted magnitudes (Table 4) shows that the predicted events closely follow the observed seismic patterns, particularly for magnitudes between 4.0 and 6.0. This agreement suggests that the model effectively learned complex, nonlinear dependencies among spatial, temporal, and geological variables, enabling it to generate realistic earthquake characteristics within the limits of the available data.

Further validation using statistical indicators confirmed that the synthetic catalog preserves essential spatial and magnitude distribution properties. The comparison of annual frequency rates, spatial clustering, and magnitude–frequency relationships revealed a

consistent correspondence between the synthetic and instrumental datasets. The synthetic events reproduce the seismic activity concentrations along major tectonic provinces, including the Alborz, Zagros, and eastern Iran fault systems. This correspondence indicates that the DNN–ECBO model not only captures statistical relationships but also reflects the regional tectonic behavior of Iran, validating the model’s ability to reconstruct missing seismic information during the pre-instrumental era.

Despite these promising outcomes, several limitations must be acknowledged. First, the model is purely data-driven and does not account for the physical processes governing earthquake generation. Therefore, it cannot reproduce stress accumulation or fault rupture dynamics. Second, the training dataset is limited to post-1964 events, which constrains the model’s generalization in regions with sparse seismic observations. Third, large-magnitude earthquakes ($M \geq 6.0$) are underrepresented due to their low occurrence frequency and the completeness level of the instrumental catalog ($M_c \approx 5.0$ – 5.5). To prevent over prediction, magnitude constraints were applied, ensuring that the number of synthetic events with $M > 5.5$ remained within the range of observed counts. Consequently, the synthetic catalog should primarily be viewed as a complementary dataset for historical completeness rather than a predictive or forecasting tool.

The reconstructed catalog provides a valuable foundation for improving regional and national seismic hazard assessments. It can be incorporated into probabilistic seismic hazard analysis (PSHA), ground motion modeling, and seismic zoning studies to enhance understanding of spatial variability in seismicity, especially for data-deficient regions. Future developments should aim to integrate tectonic stress-field data, active fault geometries, and crustal deformation parameters into the learning process to improve model interpretability. Additionally, hybrid frameworks that combine deep learning with physically based earthquake simulation models could further enhance the robustness and scientific reliability of synthetic catalogs.

5. CONCLUSION

This study applied a Deep Neural Network optimized by the Enhanced Colliding Bodies Optimization (ECBO) algorithm to reconstruct missing earthquake records in Iran between 1900 and 1963. The model, trained on post-1964 instrumental data, successfully reproduced the magnitude distributions of Iranian seismicity with low prediction errors (MAE = 0.0081, RMSE = 0.3748). Quantitative validation using Moran’s I and Kolmogorov–Smirnov tests confirmed that the synthetic catalog exhibits spatial clustering and depth distributions consistent with observed seismicity, particularly along the Alborz, Zagros, and eastern Iran fault systems. By enforcing magnitude-completeness thresholds ($M_c \approx 5.0$ – 5.5), the model avoided over prediction of large-magnitude events and maintained physical realism. The resulting synthetic catalog provides a valuable supplementary dataset for probabilistic seismic hazard analysis (PSHA), seismic zoning, and structural design in data-poor regions. Although uncertainties remain due to limited historical observations, the DNN–ECBO framework demonstrates strong potential as a data-driven approach to reconstructing pre-instrumental seismicity. Future studies should explore hybrid models combining deep learning with tectonic and geological constraints to further improve predictive reliability.

REFERENCES

1. Kaveh A. *Applications of Artificial Neural Networks and Machine Learning in Civil Engineering*. Springer Nature Switzerland; 2024.
2. Kaveh A, Biabani Hamedani K, Hosseini SM, Bakhshpoori T. Optimal design of planar steel frame structures utilizing meta-heuristic optimization algorithms. *Structures*. 2020;**25**:335–46.
3. Kaveh A, Khavaninzadeh N. Efficient training of two ANNs using four meta-heuristic algorithms for predicting the FRP strength. *Structures*. 2023;**52**:256–72.
4. Kaveh A, Akbari H, Hosseini SM. Plasma generation optimization: a new physically-based metaheuristic algorithm for solving constrained optimization problems. *Eng Comput*. 2021;**38**(4):1554–606.
5. Berberian M. *Earthquakes and Coseismic Surface Faulting on the Iranian Plateau: A Historical, Social and Physical Approach*. Elsevier; 2014.
6. Gholizadeh A, Arjmandzadeh M. Application of machine learning techniques in seismic hazard assessment. *Geosci Front*. 2019;**6**(10):1955–65.
7. Mousavi SM, Ellsworth WL, Zhu W, Chuang LY, Beroza GC. Earthquake transformer—an attentive deep-learning model for simultaneous earthquake detection and phase picking. *Nat Commun*. 2020;**11**.
8. Hosseini M, Zare M, Ansari A. Earthquake prediction using artificial neural networks: a case study in the Alborz region. *Soil Dyn Earthq Eng*. 2020;**132**:105–20.
9. Ambraseys N, Melville C. *A History of Persian Earthquakes*. 1982.
10. Ambraseys N. Engineering seismology: Part II. *Int Assoc Earthq Eng*. 1988;**17**(1):51–105.
11. Zare M, Moinfar AA. Comment on “The Rudbar-Tarom earthquake of 20 June 1990...” *Bull Seismol Soc Am*. 1994;**84**(2):484–85.
12. Mirzaei N, Gheitanchi MR. Seismotectonics of Sahneh fault, middle segment of main recent fault, Zagros mountains, western Iran. *J Earth Space Phys*. 2002;**28**(2):1–8.
13. Berberian M. *Contribution to the Seismotectonics of Iran (Part III)*. 1977.
14. Cohen GH, Karnik AR. *Synthesis of Distributed Systems – Final Report*. 1969.
15. Nowroozi AA. Seismotectonic provinces of Iran. *Bull Seismol Soc Am*. 1976;**66**(4):1249–76.
16. Seyed-Nabavi M. Seismic activity of Iran 1971–1976. *J Earth Space Phys*. 1978;**6**:38–86.
17. Engdahl ER, Jackson JA, Myers SC, Bergman EA, Priestley K. Relocation and assessment of seismicity in the Iran region. *Geophys J Int*. 2006;**167**(2):761–78.
18. Kaveh A, Mahdavi VR. Colliding bodies optimization: a novel meta-heuristic method. *Comput Struct*. 2014;**139**:18–27.
19. Kaveh A, Ilchi Ghazaan M. Enhanced colliding bodies optimization for design problems with continuous and discrete variables. *Adv Eng Softw*. 2014;**77**:66–75.

20. Kaveh A, Iranmanesh A. Structural optimization by gradient-based neural networks. *Int J Numer Methods Eng.* 1999;**46**:297–311.
21. Kaveh A, Mahdavi VR, Kamalinejad M. Optimal design of the monopole structures using CBO and ECBO algorithms. *Period Polytech Civ Eng.* 2017;**61**(1):110–16.